Experimental Studies to Verify the Efficacy of Earthquake Resistant Measures in Brick Masonry Buildings

R. N. Dubey, D. K. Paul & S. K. Thakkar
Department of Earthquake Engineering, IIT Roorkee, Roorkee -247 667, Uttarakhand, India

SUMMARY:
In the present study, seismic behaviour of conventional brick masonry construction has been studied and the adequacy of Indian Standard (IS) codal provisions for seismic zone V pertaining to earthquake resistant construction have been examined. For this purpose, conventional and earthquake resistant brick masonry models have been simultaneously tested on shock table to ensure that the base motion is same, thereby enabling a more meaningful study and to reinforce the confidence of user and builders in various provisions of seismic codes. An effort has also been made to correlate the dynamic characteristics of shock induced base motion with those of real earthquake ground motion on the basis of effective peak acceleration, frequency content, strong motion duration and destructiveness damage potential factor to examine the applicability of shock table test results to earthquake. Results demonstrate the adequacy of earthquake resistant measures in brick masonry models for earthquakes comparable to Uttarkashi earthquake.

Keywords: Brick masonry buildings, Shock table testing, IS code provisions, Earthquake resistant features

1. INTRODUCTION

Field observations during several past earthquakes have brought out the fact that a large proportion of masonry buildings collapse (or, get severely damaged) leading to enormous economic losses as well as high rate of human causality even during moderate shaking. These killer buildings are usually built using the locally available materials such as mud, bricks, stones or blocks and laid in mud, lime or cement sand mortar by local artisans who may not be familiar with the relatively newer techniques, which are meant to improve the seismic performance of such constructions. Inspite of the provisions and recommendations of the various codes, the techniques are rarely implemented in actual practice. To reinforce the confidence of the users and builders in various provisions of seismic codes, there was a need to test the conventional model as well as the model with earthquake resistant (ER) features together under the same intensity of shaking.

Tests have been conducted on half-scale models of one storeyed brick masonry building with and without earthquake resistant measures simultaneously under increasing intensity of shaking to eliminate the uncertainty of base motion parameters and the aberrations resulting from the same. Behaviour of the models including pattern of cracking, identification of weak zones, mode of failure and damage with increasing shaking have been studied and are presented herein.

2. BRICK MASONRY MODELS

For purpose of carrying out tests on shock table for studying the efficacy of IS code provisions of earthquake resistance under shock loadings, two half scale (inner plan dimensions-1.8m x 2.25m, height-1.5m and wall thickness-0.115m) brick masonry models (Fig. 2.1) were constructed and tested simultaneously on the shock table. Out of these two models, one would (Model 1) represent a single room house built in traditional way (Fig. 2.1a) without any earthquake resistant features. The other model (Model 2) was constructed with the earthquake resistant features (Fig. 2.1b) as recommended in Indian Standard codes of practice (IS: 4326-1993) for seismic zone V. The details of the two models are given in Table 2.1.

Table 2.1. Details of Brick Masonry Models

Sr. No.	Scale of Model	Earthquake Resistant Features in the Model
Model 1	Half size	Traditional brick masonry model in 1:6 cement sand mortar without any earthquake resistant (ER) features
Model 2	Half size	Earthquake resistant brick masonry model in 1:6 cement sand mortar with features such as vertical steel at the corners and the openings of jambs and seismic band at lintel level

Model 1 was constructed in a traditional manner without any features of earthquake resistant construction (Fig. 2.1a). Half scale bricks were laid using English bond in 1:6 cement sand mortar for traditional model and construction was completed providing openings for window on three sides (North, South and West) and door on the east side (Fig. 2.1a).

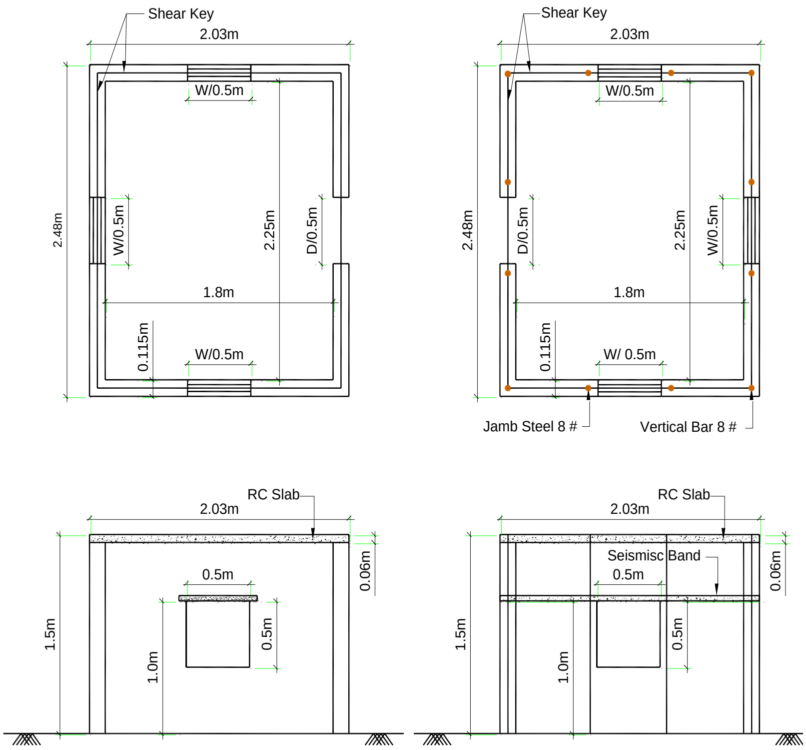

(a) Traditional model (b) Earthquake resistant model

Figure 2.1. Plan and elevation of half scale brick masonry models (Model 1 and 2)

In Model 2, all the earthquake resistant features were incorporated including vertical reinforcing bars at the corners and jambs of openings as well as seismic band (Fig. 2.2b) at the lintel level as per the guidelines given in the code of practice (IS: 4326-1993). Firstly, the corner and jamb steel of 8ϕ was welded at the base at the desired locations. Half scale bricks were laid in 1:6 cement sand mortar providing space for vertical steel bars at the corners and the openings. For full integrity of walls, horizontal seismic band was provided over all four walls at the lintel level so as to impart horizontal bending strength in them. Width of R.C. band was same as the thickness of wall (115 mm) and the thickness was kept at 37.5 mm with two longitudinal bars of 6ϕ running longitudinally over the walls held in position by stirrups of 6 mm dia spaced at 150 mm apart. Concrete mix of M15 grade was used to cast the band. The roof slab was cast as in case of traditional model.

(a) Traditional brick masonry model (b) Earthquake resistant brick masonry model

Figure 2.2. Completely constructed brick masonry models

3. SHOCK TABLE TESTING

A low cost railway wagon shock table test facility, developed by Keightly (1977), is available at the Department of Earthquake Engineering, IIT Roorkee, India for dynamic tests on structural models up to 20 tonnes weight capacity. Shock table facility (Figs. 3.1 & 3.2) comprises of (i) 36 m long track or permanent way with pre-stressed concrete (PSC) sleepers, (ii) shock table/ central wagon (7.0 m x 6.0 m) for carrying the models, (iii) one dead load wagon on each end for striking and rebound, (iv) end springs and (v) winch mechanism to pull the wagons. Shock table testing envisages testing of models under impulse type motion. The testing procedure consists of imparting shocks of gradually increasing intensity to the platform using a heavily loaded end wagon. One single shock imparts half-sine type of pulse to model bases. If another wagon on the other side is used to take reaction, another half sine pulse can be imparted from rebound. In this way one impact of end wagon can produce series of half-sine pulses. The duration of the main shock varies between 0.1 to more than 0.5 sec and peak acceleration of shock could be in the range of 0.5g to 10.0g depending upon the stiffness of end springs and weight of striking wagon.

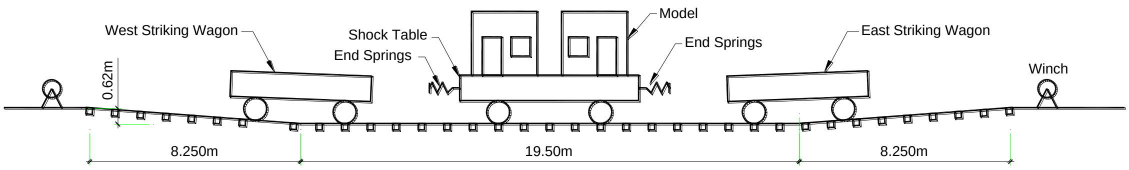

Figure 3.1. Schematic diagram of shock table facility

Figure 3.2. Shock table test facility showing the shock table and loaded end wagons

4. CORRELATION OF SHOCK MOTION WITH EARTHQUAKE GROUND MOTION

A correlation of shock induced base motion of high peak acceleration and frequency and of comparatively low duration with the equivalent earthquake ground motion is presented. Tests show unusually high base accelerations sustained by the models. As such peak base acceleration is not found to be a good indicator of damage potential of shock induced base motion, the damage characteristics of shock table motion have been compared with those of representative earthquake ground motion. Shock table motions are basically impulse type of motion with characteristics of low duration, high base acceleration and high frequency content, as compared to earthquake ground motion. Thus, it is difficult to correlate the behaviour of the structure under the shock induced motion with the earthquake motion because of its different dynamic characteristics. An effort has been made here to correlate the results obtained from the shock table motion with the earthquake motion, by considering the motion parameters, such as peak base acceleration, effective peak acceleration, strong motion duration and frequency contents. This would enable interpretation of dynamic characteristics of the shocks in terms of damage to be expected in real earthquake motion.

4.1. Damage potential characterization of ground motion

Uang and Bertero (1988) have summarized the various parameters to characterize the damage potential of strong shaking.

Earthquake intensity denoted by I_A has been defined by Arias (1970), as sum of total energy per unit mass stored in the oscillators of a population of undamped linear oscillators uniformly distributed with respect to their frequencies, at the end of the strong motion duration as

$$I_A = \frac{\pi}{2g}\int_0^{t_d} \ddot{V}_g^2(t)\,dt = \frac{1}{2g}\int_0^{\infty} \left| F_{\ddot{V}_g}(\overline{\omega}) \right|^2 d\overline{\omega} \tag{4.1}$$

where t_d and $\ddot{V}_g(t)$ are the total duration and ground acceleration of an earthquake respectively and $\left| F_{\ddot{V}_g}(\overline{\omega}) \right|$ is the Fourier amplitude of $\ddot{V}_g(t)$.

Earthquake Power has been proposed by Housner (1975), as a measure of damage potential P_A given by

$$P_A = \frac{1}{(t_{0.95} - t_{0.05})}\int_{t_{0.05}}^{t_{0.95}} \ddot{V}_g^2(t)\,dt \tag{4.2}$$

where $t_{0.05}$ and $t_{0.95}$ are the time instants at which I_A have 5% and 95% values, respectively. One commonly used definition of strong motion duration t_D is given by Trifunac and Brady (1975)

$$t_D = t_{0.95} - t_{0.05} \tag{4.3}$$

Elastic Response Spectrum Intensity (SI) has been proposed Housner (1952) as

$$SI\,(\xi) = \int_{0.1}^{2.5} S_{pv}(\xi, T)\,dT = \frac{1}{2\pi}\int_{0.1}^{2.5} S_{pa}(\xi, T)\,T\,dT \tag{4.4}$$

where, T is the period of single degree of freedom system, S_{pv} is the linear elastic pseudo-velocity, S_{pa} is the linear elastic pseudo-acceleration and ξ is the damping ratio (taken as 5%).

Araya and Saragoni (1985) have simultaneously accounted for the effect of maximum ground acceleration, duration and frequency content of strong motion in defining destructiveness damage potential factor as

$$P_d = \frac{I_A}{\mu_0^2} \tag{4.5}$$

where, I_A is the intensity which covers maximum ground acceleration and strong motion duration and μ_0 is the intensity of zero crossing which envelops frequency content.

Characteristic frequency f_0 is calculated as zero up-crossing rate of the base motion for the duration considered.

Realizing the shortcoming of using peak instrumental values, ATC (1978) introduced the concept of effective peak acceleration. Although effective peak acceleration is a philosophically sound parameter for seismic hazard analysis, at present there is no standardized definition of this parameter. ATC defines the effective peak acceleration (EPA) as follows:

$$EPA = \frac{\overline{S}_{pa}}{2.5} \tag{4.6}$$

where, $\overline{S}_{pa}$ the mean pseudo-acceleration value is in the period range of 0.1 to 0.5 sec for the 5% damped linear elastic response spectrum.

Out of five parameters defined above, Araya's destructiveness damage potential factor, P_d is considered to have greater merit in reflecting the damage potential of the motion. Destructiveness damage potential factor considers intensity, duration and frequency content simultaneously. It is believed that this type of approach will give a more meaningful measurement of damage potential due to shock table motion in correlating with earthquake ground motion and comparing the damages observed during shock table testing and actual damages in earthquake ground motion.

To interpret the results of shock table tests in terms of the expected damage due to earthquake ground motion, a comparison of the various base motion parameters of the shocks has been made with the ground motion parameters of a recorded Indian earthquake namely, Uttarkashi (Fig. 4.1).

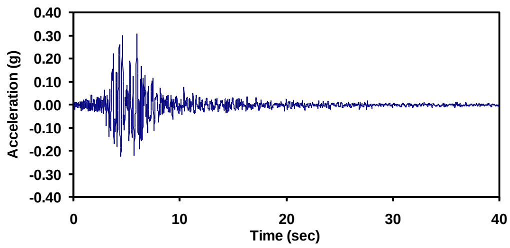

Figure 4.1. Acceleration time history of Uttarkashi earthquake of Oct. 20, 1991 recorded at Uttarkashi, India, component: N75E

5. BEHAVIOUR OF MODELS DURING SHOCK LOADINGS

When building models are subjected to impulse type of loading, inertia forces, proportional to the masses of the models are induced. Since the shock loading is in longitudinal direction, horizontal inertia forces will be acting on the models, resulting in the vibration of the buildings. The structural elements, which were basically carrying vertical loads before the shock, have to carry lateral loads as well, causing additional bending and shearing effects.

5.1. Behaviour of model 1 during first, second and third shock

Depending on the experience of testing of previous masonry models on shock table, the brick masonry models (Model 1 and 2) were subjected to shock from the scaled mark position on the west side of the railway track. The peak base acceleration (PBA) imparted to platform at the base was of the order of

0.53g (Fig. 5.1). The maximum roof acceleration of this model was observed to be 0.59g. The shock was not so intense as to cause any damage to the conventional model (Model 1).

In the second and the third shock, there was a gradual increase in the intensity of the loading. The peak base acceleration was recorded as 0.89g (Fig. 5.1) and 1.18g (Fig. 5.2) respectively. There was no damage to the traditional model.

5.2. Behaviour of model 2 during first, second and third shock

Earthquake resistant brick masonry model (Model 2) also experienced the same base motion as that of traditional brick masonry model (Model 1) during first, second and third shock. Model 2 was also undamaged and the maximum roof acceleration was observed to be 0.61g, 1.1g and 1.56g respectively. It was noticeable from the increase in the roof accelerations of the Model 1 and 2 that the earthquake resistant model was stiffer than the traditional model and that is why the amplification was more in earthquake resistant model (Model 2). This verified the fact that earthquake resistant features incorporated in the model have contributed significantly in increasing the stiffness of the model.

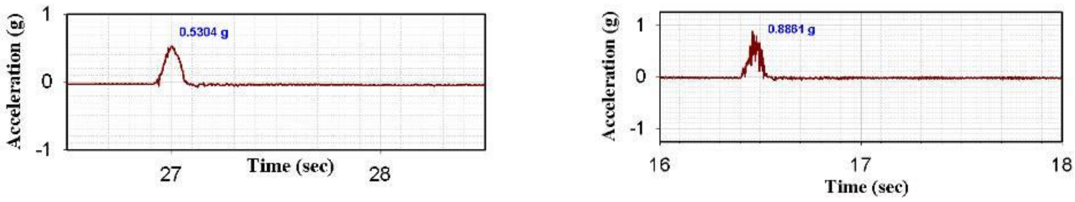

Figure 5.1. Acceleration time history at the base of central wagon after shock 1 & 2 respectively

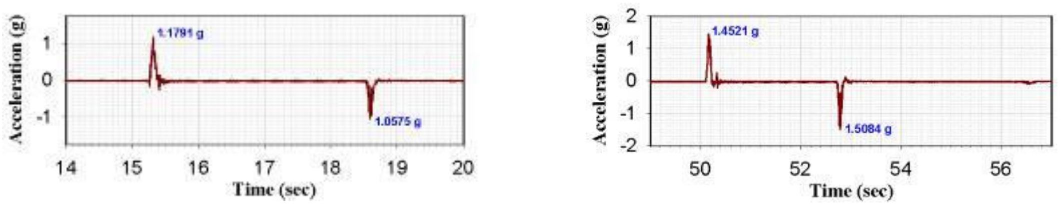

Figure 5.2. Acceleration time history at the base of central wagon after shock 3 & 4 respectively

5.3. Behaviour of model 1 during fourth shock

During fourth shock there was further increase in the intensity of the impact and the peak base acceleration was recorded as 1.45g in the loading cycle and 1.51g (Fig. 5.2) in the rebound cycle. The roof acceleration in the traditional model (Model 1) was recorded as 1.24g in the loading shock and 1.38g in the rebound action. Decrease in the roof acceleration was quite evident as the traditional model developed visible cracks in all the four walls including bending (east and west cross) walls and shear (south and north) walls. Horizontal bending cracks in the west cross wall at the foundation level and near the window opening spreading up to the corner of wall were clearly visible (Fig. 5.3). Shear walls on the northern and southern sides (Fig. 5.4) developed diagonal shear cracks originating from window openings and spreading to the corners of the wall.

Figure 5.3. Damage to bending (cross) walls of Model 1 on west and east side after shock 4

Figure 5.4. Damage to shear walls of Model 1 on south and north side after shock 4

5.4. Behaviour of model 2 during fourth shock

For the same base motion as in fourth shock, which was imparted to Model 1, the earthquake resistant model (Model 2) was intact. The roof motion was amplified by 29.5% from 1.45g to 1.88g in the loading cycle. The earthquake resistant features viz. seismic band at lintel level, vertical corner steel and jamb steel near four openings worked effectively providing box action and proper anchorage of walls with foundation and roof.

5.5. Behaviour of model 1 during fifth shock

Fifth shock was given with further increase in the intensity of the impact and the peak base acceleration was observed to be 1.93g in the loading cycle and 1.62g (Fig. 5.5) in the rebound cycle. The maximum roof acceleration in the traditional model (Model 1) was recorded as 0.51g in the loading shock and 0.88g in the rebound cycle. Quite obviously the roof motion of the Model 1 decreased as compared to base motion. Severe and wide spread cracks were seen in the traditional brick masonry model (Fig. 5.6).

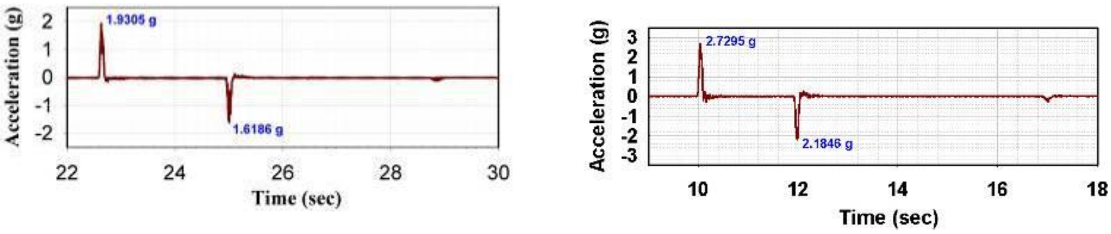

Figure 5.5. Acceleration time history at the base of central wagon after shock 5 & 6 respectively

Figure 5.6. Damage to cross and shear walls of Model 1 after shock 5

5.6. Behaviour of model 2 during fifth shock

The earthquake resistant model experienced similar base motion as that of Model 1 (1.93g) in the loading cycle and 1.62g in the rebound pulse. The maximum roof acceleration in Model 2 was observed to be 2.02g in the loading cycle and 1.84g in the rebound pulse. Obviously, the model showed much improved behaviour since the walls were tied together by the means of rigid reinforced concrete slabs and horizontal seismic band at lintel level and vertical steel.

5.7. Behaviour of model 1 during sixth shock

In the sixth shock, the intensity of loading was further increased and the peak base acceleration was recorded as 2.73g in the loading cycle and 2.18g (Fig. 5.5) in rebound cycle. Because of the damaged condition of the traditional model after the fifth shock, the model was likely to collapse and it finally did (Fig. 5.7). During the sixth shock, peak base acceleration was more than 5 times as compared to the base motion in the first shock.

Figure 5.7. Collapse of Model 1 and minor damage to south shear wall of Model 2 after shock 6

5.8. Behaviour of model 2 during sixth, seventh and eighth shock

During the sixth shock, roof acceleration was recorded as 2.90g in the loading cycle and 2.62g in the rebound pulse. There was a minor damage to the model with earthquake resistant features during this shock. Horizontal cracks originating from the window opening appeared on the northern and southern shear walls (Fig. 5.7). There was no damage to the east and west cross (bending) walls.

During the seventh shock, the peak base acceleration was recorded as 3.38g in the loading cycle and 3.35g in rebound pulse. There was moderate damage to the model with earthquake resistant features during this shock. Horizontal cracks originating from the window openings widened and some new cracks were also seen. Diagonal shear cracks were also observed on the north and south shear walls (Fig. 5.8). Vertical cracks appeared at the corners of the walls. Horizontal cracks were seen on the east and west cross walls.

Intensity of loading was further increased during eighth shock. The peak base acceleration was recorded as 4.52g in the loading cycle. The damage to the model increased in all the four walls. Horizontal cracks originating from the window openings further widened and some new cracks were seen. Severe diagonal shear cracks were also observed on the north and south shear walls and few pieces of bricks fell down from the corners of window openings (Fig. 5.8). Vertical cracks appeared at the corners of the walls. Many new horizontal cracks developed on the east and west cross walls because of the intense base motion of the order of 4.52g which was more than eight times of the base motion during shock 1. But the earthquake resistant features helped to withstand the severe shocks without collapse.

Figure 5.8. Damage to south shear wall of Model 2 after shock 7 & 8 respectively

6. SHOCK INDUCED MOTION AND EARTHQUAKE GROUND MOTION

A total of eight shocks were imparted to the models. The peak base acceleration was varied from 0.53g in first shock to 4.52g in the eighth shock (Table 6.1) in the loading cycle. It has been observed that destructiveness damage potential factor (Table 6.2) is the only reasonable parameter that correlates the shock table motion with earthquake ground motion. Shock 8 with PGA value as high as 4.52g, has destructiveness damage potential factor (0.79) similar to that of Uttarkashi earthquake (0.81).

Table 6.1. Comparison of Behaviour Of The Two Models After Shock Loading

Shock No.	Base Acceleration (g)		Model 1 (Traditional Model)		Model 2 (ER Model)	
	Loading pulse	Rebound pulse	Roof Acceleration (g)	Behaviour of Model 1	Roof Acceleration (g)	Behaviour of Model 2
1	0.53	-	0.59	No cracks	0.61	No cracks
2	0.89	-	0.91	No cracks	1.10	No cracks
3	1.18	1.10	1.14	No visible damage	1.56	No cracks
4	1.45	1.51	1.24	Moderate damage	1.88	No cracks
5	1.93	1.62	0.51	Severe damage	2.02	No cracks
6	2.73	2.18	-	Collapsed	2.90	Minor cracks
7	3.38	3.35	-	Collapsed	3.85	Moderate cracks
8	4.52	4.05	-	Collapsed	4.60	Severe cracks

Table 6.2. Comparison Of Earthquake Ground Motion Parameters With Shock Table Motion Imparted To Brick Masonry Models

Shock table motion/ Earthquake	PGA/ PBA (g)	EPA (ATC) (g)	I_A (10^{-1} g.sec)	t_D (sec)	f_0 (Hz)	P_A (10^{-2} g^2)	SI (10^{-1} g.sec^2)	P_d (10^{-3} g.sec^3)
Shock-1	0.53	0.15	0.25	0.075	8.33	18.02	0.549	0.09
Shock-2	0.89	0.16	0.36	0.075	19.51	28.97	0.632	0.11
Shock-3	1.18	0.25	0.75	0.085	20.51	60.68	0.843	0.19
Shock-4	1.45	0.34	1.40	0.090	23.53	123.11	1.376	0.23
Shock-5	1.93	0.39	1.91	0.095	21.05	166.43	1.793	0.32
Shock-6	2.73	0.68	5.24	0.010	14.12	492.42	2.505	0.51
Shock-7	3.38	0.80	9.53	0.105	12.16	524.89	3.215	0.67
Shock-8	4.52	0.84	10.45	0.110	12.56	580.69	3.350	0.79
Uttarkashi	0.31	0.21	0.98	6.880	5.50	0.822	0.584	0.81

7. CONCLUSIONS

Based on the foregoing experimental studies on seismic behaviour of brick masonry buildings, some specific conclusions drawn are as follows:

(i) The models were imparted shock induced motion by striking wagon with increasing intensity. The peak base acceleration (PBA) of the platform varied from 0.53g (shock 1) to 4.52g (shock 8). As peak base accelerations are not found to be a good indicator of damage potential of shock induced motions, damage characteristics of shock induced motion have been compared with those of actual earthquake ground motion. The effective peak accelerations (EPA) of all the eight shocks varied from 0.15g to 0.84g respectively for 5% damped linear response spectrum. The traditional model started developing fine cracks from shock 3 onwards which increased during shock 4 and 5 and finally collapsed during shock 6.

(ii) The failure occurred due to development of diagonal cracks starting from window openings in the shear walls (i.e. walls parallel to shock loading). The walls normal to shock loading developed horizontal cracks at the base and at sill level due to bending tension and then started sliding at the mortar joint due to shear.

(iii) The destructiveness damage potential factor of the shock induced base motions varied from 0.09 (shock 1) to 0.79 (shock 8). Further, it can be seen that destructiveness damage potential factor of shock 8 was equivalent to that of Uttarkashi earthquake (0.81). The patterns of damage in the traditional brick masonry model in the shock induced motion were also in agreement with damage observed during Uttarkashi earthquake.

(iv) Earthquake resistant elements incorporated in the earthquake resistant (ER) model in the form of vertical steel and seismic band have led to significant improvement in its performance. It showed only partial damage even during shock 8 while the traditional model collapsed during shock 6 itself. The model has undergone minor damage but could very well sustain shock similar to Uttarkashi earthquake.

(v) The comprehensive experimental study, using relatively modest testing facility, has demonstrated a clear enhancement in the seismic competence introduced by the codal provisions incorporated in the model, providing an explicit verification of the codal provisions of IS: 4326-1993. The series of experiments show and suggest that the codal provisions for the masonry buildings are effective in resisting strong motion earthquakes like the one in Uttarkashi (1991). The tests also serve to reinforce the confidence of the users and builders in the various provisions of the seismic codes.

ACKNOWLEDGEMENT
The study was supported by the Disaster Mitigation Division of Ministry of Home Affairs, Govt. of India, New Delhi. Authors thankfully acknowledge the financial support received from the Ministry.

REFERENCES

Arias, A. (1970). A measure of earthquake intensity. *Seismic Design for Nuclear Power Plants*. ed. R.J. Hansen, Massachusetts Institute of Technology Press, Cambridge, Mass. pp 438-469.

Araya, R. and Saragoni, G.R. (1985). Earthquake accelerogram destructiveness potential factor. *Proceedings of Eighth World Conference on Earthquake Engineering*. EERI, San Francisco, CA. pp 835-842.

Applied Technology Council. (1978). Tentative provisions for the development of seismic regulations for buildings. *U.S. National Bureau of Standards*. Special Publication 510.

Dubey, R.N. (2011). Experimental studies to verify the efficacy of earthquake resistant measures in masonry buildings. Ph.D. Thesis, *Department of Earthquake Engineering*. IIT Roorkee, Roorkee.

Housner, G.W. (1952). Spectrum intensities of strong motion earthquakes. *Proceedings of the Symposium of Earthquake and Blast Effects on Structures*. EERI, Los Angeles, California. pp 21-36.

Housner, G.W. (1975). Measure of severity of earthquake ground shaking. *Proceedings of the U.S. National Conference on Earthquake Engineering*. EERI, Ann Arbor, Michigan. pp 25-33.

IS: 13828 (1993). Improving earthquake resistance of low strength masonry buildings – Guidelines. *Bureau of Indian Standard.* New Delhi.

IS: 4326 (1993). Indian standard code of practice for earthquake resistant design of buildings. *Bureau of Indian Standard.* New Delhi.

Keightley, W.O. (1977). Report on Indo-U.S. subcommission on education & culture. *Department of Earthquake Engineering.* University of Roorkee, Roorkee.

Trifunac, M.D. and Brady, A.G. (1975). A study on the study of strong earthquake ground motion. *Bulletin of the Seismological Society of America*. **Vol. 65**, No. 3, pp 581-626.

Uang, Chia-Ming. and Bertero, V.V. (1988). Implications of recorded earthquake ground motions on seismic design of building structures. *Report No. UCB/ EERC-88/13,* University of California, Berkeley, CA.